Accepted Manuscript online: 2023-02-23 Article published online: 2023-04-03

[4 + 4]-Imine Cage Compounds with Nitrogen-Rich Cavities and Tetrahedral Geometry

Ke Tian[§, a]
Xubin Wang[§, a]
Moritz P. Schuldt[a]
Sven M. Elbert[a]
Frank Rominger[a]
Michael Mastalerz[* a]

[a] Organisch-Chemisches Institut, Ruprecht-Karls-Universität Heidelberg, Im Neuenheimer Feld 270, 69120 Heidelberg, Germany
[§] These authors contributed equally to this work.
[*] michael.mastalerz@oci.uni-heidelberg.de

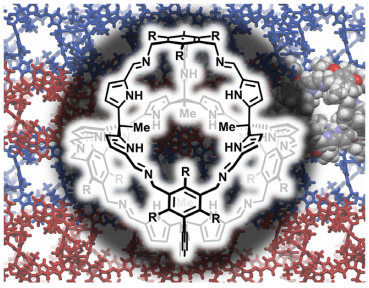

Received: 07.10.2022
Accepted after revision: 15.02.2023
DOI: 10.1055/a-2041-5362; Art ID: OM-2022-10-0040-SC

Abstract Organic imine cage compounds have found a variety of different applications in several fields in materials science. To design tailor-made cages for corresponding applications, synthetic approaches to cages with tunable functionalities, sizes and shapes have to be found. Here we report a series of cages with truncated cubic shape and tetrahedral geometry possessing nitrogen-rich cavities.

Key words: organic cage compounds, imines, pyrrols, dynamic covalent chemistry

Introduction

Organic cage compounds have gained a lot of interest in the past decades[1–5] due to emerging applications in materials science. They found their use in sensor films,[6] as coatings for quartz crystal microbalances,[7,8] for selective ion recognition,[9] to make porous membranes,[10,11] for selective gas sorption[12–15] and separation,[16–20] catalysis,[21] or as stationary phases for gas chromatography.[22,23] To create cages for specific applications it is important to control parameters such as size,[24] shape,[25] geometry[3,4] as well as number and positions of functional groups.[9,26] Most cage compounds are synthesized by dynamic covalent chemistry (DCC).[27] Among DCC reactions, the reactions forming boronic acid esters or imines are the most common ones and for the latter a huge variety of geometries such as (truncated)[28,29] tetrahedra,[30–33] trigonal prisms,[34–36] cubes,[16,37,38] rhombicuboctahedra,[39–41] adamantoids,[35,42,43] tetrapods,[44] cucurbitimines[45] or more complex structures such as catenanes[46,47] have been realized and some of these structures have even been post-stabilized to enhance their chemical robustness.[6,48–50] Cages with nitrogen-containing pyridine[9,51] or pyrrol-units[52] showed superior behavior in, e.g., ion recognition and could act as ligands for several transition metal ions as shown for numerous metal–organic cage compounds or complexes.[53,54] To extend the portfolio of organic cage compounds, we envisioned the synthesis of tetrahedral [4 + 4] imine cages, which are based on a *tris*pyrrol aldehyde, a unit used by Beer and co-workers for flexible [2 + 3] cages,[55,56] yet this time with substituted 1,3,5-trimethylamino benzenes[9,28] to retain a higher degree of shape persistency.

Results and Discussion

The desired cage compounds were synthesized by condensation reactions of methyl-*tris*pyrrolyl-aldehyde **1**[56] with equimolar amounts of the differently substituted triamines **2-Me, 2-Et, 2-OPr** and **2-Br** in chloroform at room temperature or 60 °C (Scheme 1). Due to their solubility in common

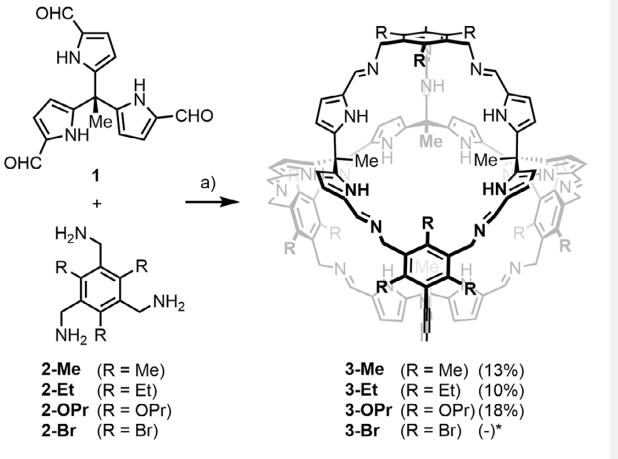

Scheme 1 Synthesis of the cage compounds. a) $CHCl_3$, TFA (3 mol-%), rt or 60 °C, 2 d.

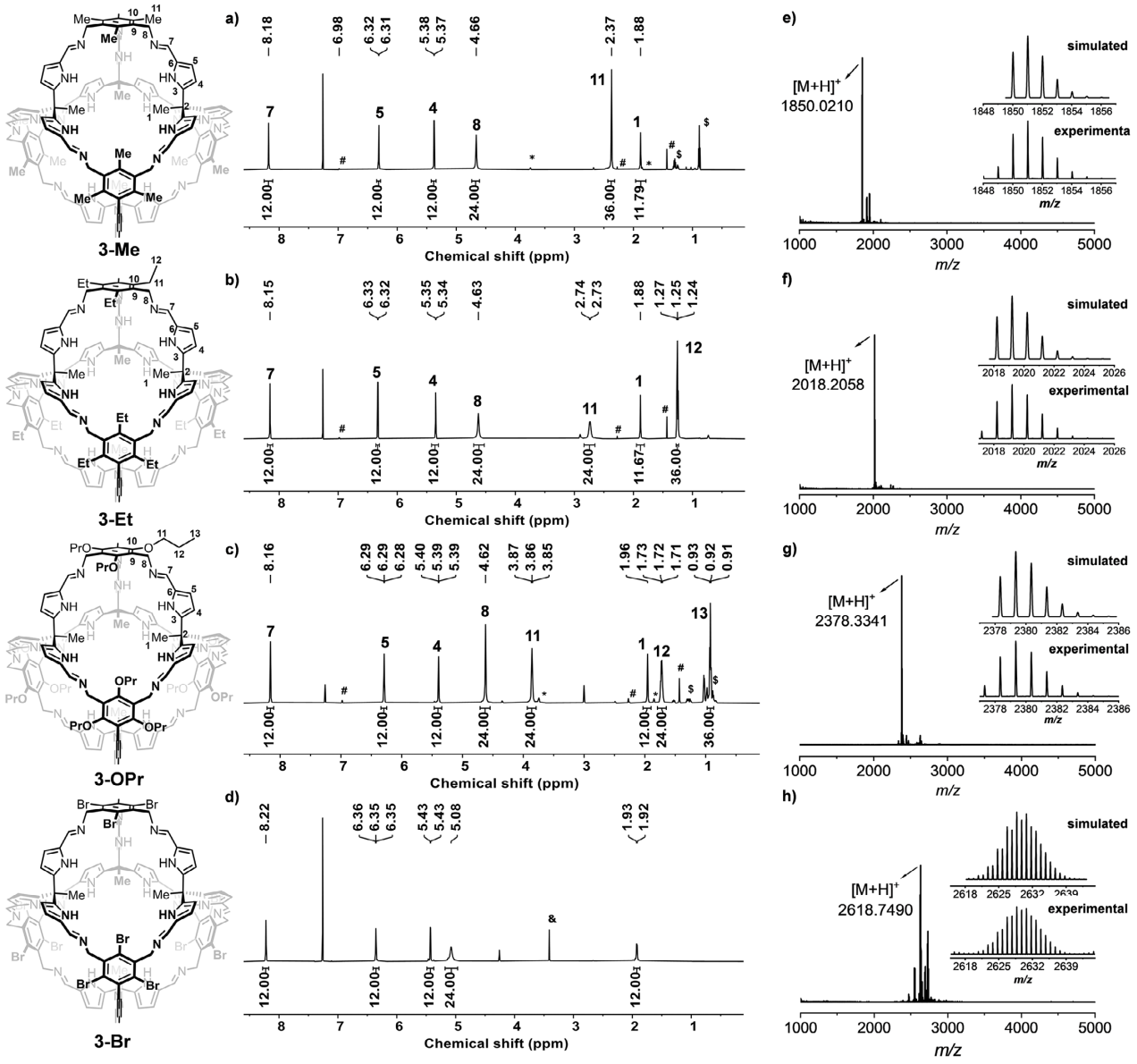

Figure 1 a – d) ^{1}H NMR spectra and of cage **3-Me** (a) (600 MHz), **3-Et** (b) (600 MHz), **3-OPr** (c) (700 MHz) and **3-Br** (d) (700 MHz) in $CDCl_3$. # = BHT, * = THF, $ = pentane, & = methanol. e – h) MALDI-TOF mass spectra (matrix: DCTB) of **3-Me** (a), **3-Et** (b), 3-**OPr** (c) and **3-Br** (d). Simulated (top) and experimental (bottom) isotopic patterns are shown as insets.

organic solvents, cage compounds **3-Me, 3-Et** and **3-OPr** were successfully isolated by recycling gel permeation chromatography (rec-GPC) in THF after 6 (**3-Me** and **3-Et**) or 15 (**3-OPr**) recycling cycles in yields between 10 and 18% (for chromatograms, see the Supporting Information, SI).

Due to its low solubility, the purification of **3-Br** by rec-GPC was not possible and attempts to remove impurities by recrystallization failed, so that minor impurities remained. The successful synthesis of the cages was verified by ^{1}H NMR spectroscopy by the disappearance of the signals of the aldehyde units of **1** (δ = 9.13 ppm) as well as of the amine units of **2-Me, 2-Et, 2-OPr** and **2-Br** (δ = 1.30 – 1.63 ppm). Instead, signals of the imine protons of cages **3-Me, 3-Et, 3-OPr** and **3-Br** at δ = 8.15 – 8.24 ppm were found (labeled as protons 7 in Figure 1a – d). Furthermore, MALDI-TOF mass spectrometry shows signals at *m/z* 1850.0210 (**3-Me**; calc: 1850.0201), *m/z* 2018.2058 (**3-Et**; calc: 2018.2079), *m/z* 2378.3341 (**3-OPr**; calc: 2378.3346) and *m/z* 2618.7553 (**3-**

Br; 2618.7568) representing the corresponding [4 + 4] condensates (Figure 1e – h).

The low isolated yields of cages **3-Me, 3-Et** and **3-OPr** after rec-GPC purification can be rationalized by the formation of several other species as obvious by multiple peaks in the GPC-chromatograms (see the SI). MALDI-TOF MS analyses of the isolated fractions showed the 4 + 4 condensates as main components alongside minor impurities for each fraction. Nevertheless, ^{1}H NMR analyses revealed more complex patterns leading to the hypothesis of isomeric cage structures. To get further insight into possible cage isomers, we conducted quantum chemical calculations at the B3LYP/6 – 31 G(d) level of theory and calculated the interconversion energy of a pro-chiral *tris*pyrrol unit to elucidate whether these units lead to a potential mixture of diastereoisomeric cages (Figure 2). Even considering the highest energy barrier between intermediate II and transition state III of 23.7 kJ/mol would result in a rapid interconversion rate of $4.35 \cdot 10^8 \cdot s^{-1}$ and a half-life time of 1.59 ns, suggesting a fast interconversion in solution. This is further underlined by the comparably low relative energies of *MMMM, MMMP, MMPP, MPPP* and *PPPP* cages of 6.7 to 11.1 kJ/mol independent of the side chains (see SI), indicating again a fast interconversion excluding diastereomeric cages causing the several fractions obtained by rec-GPC. Another possibility is the formation of *in–out*-isomers referring to the central methyl-units of the *tris*pyrrols. The relative energies of the possible *in–out*-combinations show that the all-*in* isomers should represent > 98.5% of the cages in a dynamic equilibrium in solution. Thus, it can be concluded that the different fractions obtained by rec-GPC contain different *in–out* isomers of the cages that are kinetically trapped.

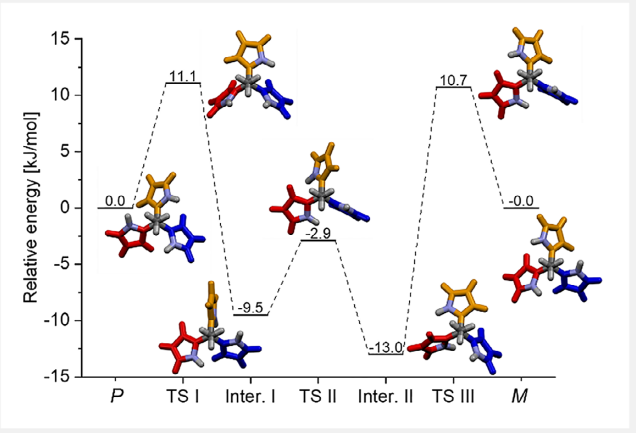

Figure 2 DFT-calculated (B3LYP/6 – 31 G(d)) interconversion of *P*- to *M*-*tris*pyrrol.

For all isolated all-*in* cages, suitable crystals for single-crystal X-ray diffraction (SCXRD) analyses have been obtained, unambiguously proving the molecular structures of the [4 + 4] cages (Figure 3). The geometrical shapes can best be described as truncated cubes with tetrahedral symmetry. In all studied cases, the central methyl group of the *tris*pyrrols is pointing into the cage cavities resulting in distances to adjacent phenyl rings of $d_{Me\text{-}Ph}$ = 1.2 – 1.3 nm and outer diameters of d = 1.5 – 1.6 nm. As previously observed, for **3-Me** all ethyl substituents are conformationally stable and point outwards, whereas propoxy groups in **3-OPr** point either out- or inwards.

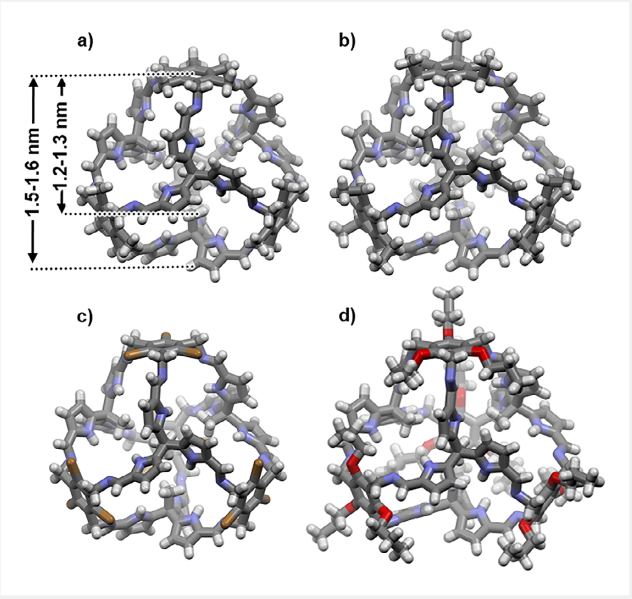

Figure 3 Single-crystal X-ray structures of the cages **3-Me, 3-Et, 3-OPr** and **3-Br** as capped-stick models. The distances of a phenyl unit to the opposing internal methyl group and to the outer carbon atoms of the *tris*pyrrol moiety are given for **3-Me** exemplarily. Colors: carbon, gray; nitrogen, blue; oxygen, red; bromine, brown; hydrogen, white.

Besides the solvate **3-Et$_\alpha$** crystallized from dichloromethane and hexane (cubic, $P_a\bar{3}$) and cage **3-OPr** (orthorhombic, $A_{ba}2$), all obtained structures crystallized in the triclinic space group $P\bar{1}$. Due to steric repulsion, each *tris*pyrrol unit adopts a chiral C_3-symmetrical conformation (for the sake of simplicity, we name them here *M* or *P* orientation), which can interconvert quickly by rotation around the C–C single bonds to the central carbon atom. Thus, each *tris*pyrrol unit is prochiral leading to overall five possible cage isomers due to their tetrahedral symmetry. The solid-state structures of **3-Me, 3-Et$_\beta$, 3-OPr** and **3-Br** adopt single enantiomeric *MMMM* or *PPPP* orientation, an effect comparable to the assembly of face-orientated polyhedra derived from prochiral building blocks as reported by Cao's group (Table 1 and Figure 5).[57,58] Since four out of eight "faces" of the synthesized truncated cubes possess helical chirality, the cages can be understood as semi-face-orientated polyhedra.

Table 1 Selected crystallographic data of cages **3-Me**, **3-Et**, **3-OPr** and **3-Br**.

Compound	Solvents	Crystal system	Space group	Z	Cell volume	Isomers observed	Packing
3-Me	$CDCl_3$/MeOH	Triclinic	$P\bar{1}$	2	7578.4 Å^3	*MMMM*/*PPPP*	Enantiopure layers
3-Et$_\alpha$	CH_2Cl_2/C_6H_{14}	Cubic	$P_a\bar{3}$	8	31 222.2 Å^3	*MMMP*/*PPPM*	3D-alternating
3-Et$_\beta$	CH_2Cl_2/MeOH	Triclinic	$P\bar{1}$	2	7646.5 Å^3	*MMMM*/*PPPP*	Enantiopure layers
3-Et$_\gamma$	$CDCl_3$	Triclinic	$P\bar{1}$	2	8142.8 Å^3	*MMMP*/*PPPM*	Enantiopure layers
3-OPr	CH_2Cl_2/MeOH	Orthorhombic	$A_{ba}\bar{2}$	4	18 567.7 Å^3	*MMMM*/*PPPP*	Enantiopure layers
3-Br	CH_2Cl_2/MeOH	Triclinic	$P\bar{1}$	2	7399.5 Å^3	*MMMM*/*PPPP*	Enantiopure layers

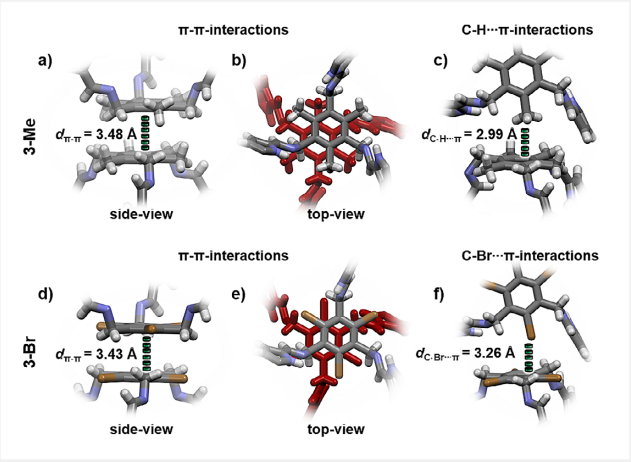

Figure 4 Intermolecular interactions found in the single-crystal X-ray structures of **3-Me** (a – c) and **3-Br** (d – f).

Cages **3-Me** and **3-Br** both pack in the triclinic space group $P\bar{1}$ in an isomorphic fashion, which is obvious for example from the comparable unit cell volumes of 7578.4 Å^3 (**3-Me**) and 7399.5 Å^3 (**3-Br**) (Table 1). In both cases face-to-face π–π-stacking motifs are found on one face of each cage with distances of $d_{\pi-\pi}$ = 3.43 Å (**3-Br**) or 3.48 Å (**3-Me**) (Figure 4). The residual faces interact, e.g., via C – H···π interactions in the case of **3-Me** with $d_{C-H\cdots\pi}$ = 2.99 Å (Figure 4c). This interaction is mimicked in **3-Br** by C–Br···π interactions of $d_{C-Br\cdots\pi}$ = 3.26 Å (Figure 4f), leading in both cases to enantiopure layers within the crystallographic *ab*-planes (Figure 5f).

Changing the solvent diffused into saturated solutions of **3-Et** from methanol (leading to **3-Et$_\beta$** with enantiopure cages) to hexane or if the crystals were grown by slow evaporation of a $CDCl_3$ solution of **3-Et**, solvates **3-Et$_\alpha$** and **3-Et$_\gamma$** are obtained showing the *MMMP* and *PPPM* isomers exclusively (Figure 5).

In the case of **3-OPr**, packing in the orthorhombic space group $A_{ba}2$, similar layers as in **3-Me** and **3-Br** are found in the crystallographic *bc*-plane with one-dimensional channels along the *c*-axis filled with methanol and water molecules (see Table 1, Figure 5, Figure 6 and discussion below). For **3-Et,** the homochiral solvate **3-Et$_\beta$,** as well heterochiral solvate **3-Et$_\gamma$**, form layered structures as well, while **3-Et$_\alpha$** crystallizes in the cubic space group $P_a\bar{3}$ and the enantiomeric cages *MMMP*-**3-Et** and *PPPM*-**3-Et** can be found in an alternating order in all three dimensions (Figure 5f).

The nitrogen-rich inside of the cages' cavities should be a perfect environment for polar guests. Crystallizing **3-Me** using $CHCl_3$ and methanol led to 12 enclathrate-ordered methanol molecules in defined H-bonded arrays interacting with the pyrrol-imine subunits via synergetic H-bonds of $d_{N-H\cdots O}$ = 2.00 Å and $d_{O-H\cdots N}$ = 2.11 Å (Figure 6a – c). This alignment generates a "shell" of methanol molecules by the interaction of the highly polar OH-groups and the inner surface of the cage leaving the methyl groups pointing to the inside of the cage creating a more nonpolar environment. Inside this nonpolar pocket, exactly one molecule of $CHCl_3$ can be found to be interacting via van-der-Waals interactions (Figure 6a).

While Russian-doll alignments with three spheres have been realized on a molecular level;[59–62] to the best of our knowledge, the structure discussed here is the first organic cage compound with two of these spheres being two different solvents. Furthermore, seven more methanol and one water molecule fill the inter-cage voids in the crystalline packing. For **3-Et$_\beta$**, 10 methanol molecules are found in similar alignments as discussed for **3-Me** (Figure 6), yet due to disorder the residual solvent molecules had to be SQUEEZED. Ten methanol molecules are also found in the cavity in **3-OPr** (Figure 6d). This time the residual voids are filled with ten water molecules which align in a chain-like fashion along the crystallographic *a*-axis (Figure 6d). Due to fast exchange, the H-atoms of the water molecules were not crystallographically found and a detailed discussion of the hydrogen bonding pattern is not possible.

Conclusions

To summarize, we have constructed four cage molecules based on a *tris*pyrroltrialdehyde. While **3-Me, 3-Et** and **3-OPr** have been successfully isolated and fully characterized, **3-Br** was mainly investigated by SCXRD. A detailed study of six single-crystal X-ray structures in total revealed that the prochiral *tris*pyrroltrialdehyde orient in homoenantiomeric

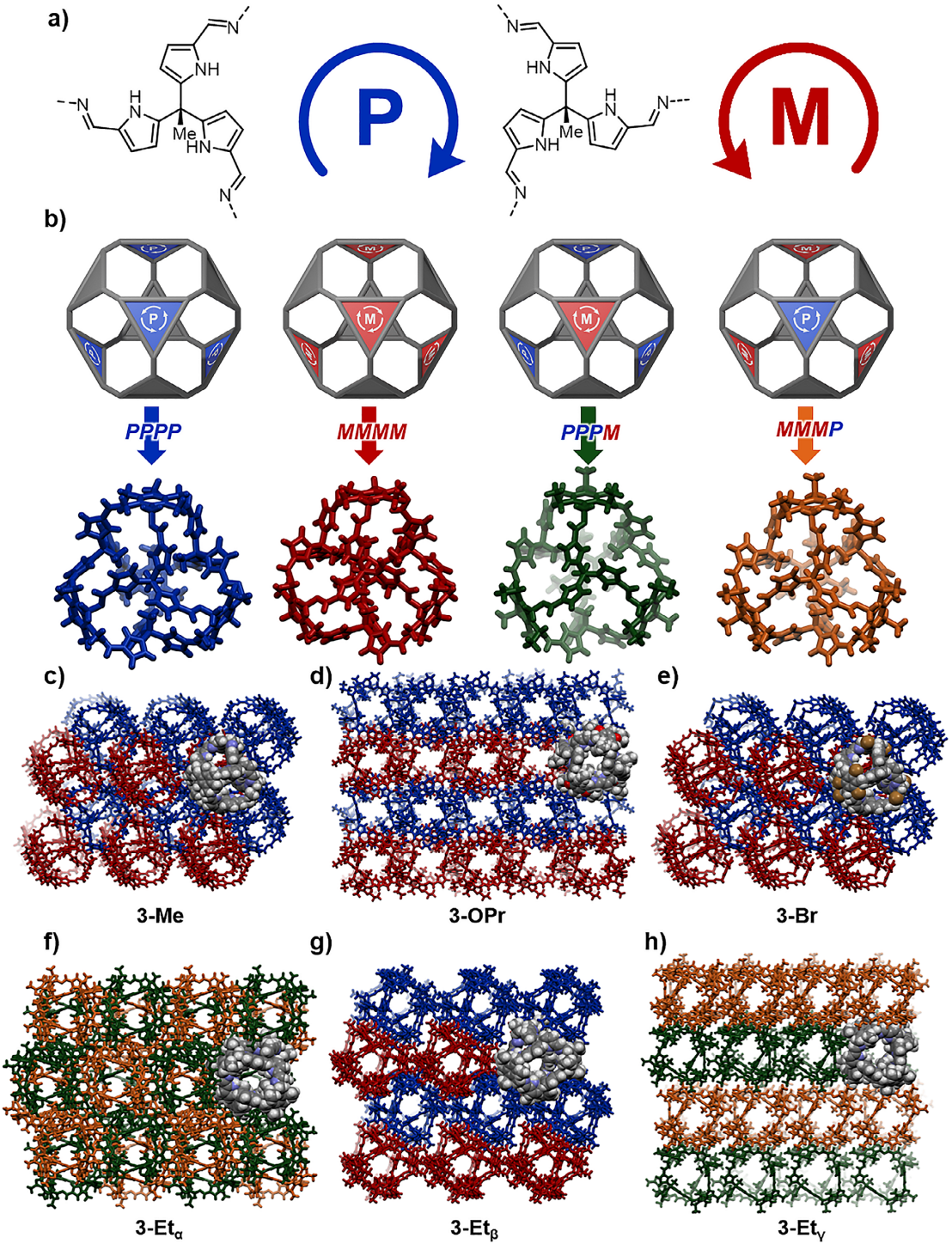

Figure 5 a) Schematical depiction of the *P*- and *M*-alignment of the prochiral *tris*pyrrol units. *Note*: The methyl group pointing out of the paper plane here is pointing inside the cage voids, which has to be taken into account in the following figures. b) Schematic representations of the homochiral *PPPP* (shown in blue for **3-Me**) and *MMMM* (shown in red for **3-Me**) as well as heterochiral *PPPM* (shown in green for **3-Et$_\alpha$**) and *MMMP* (shown in orange for **3-Et$_\alpha$**) cages. d – h) Packing motifs of the obtained solvates with different enantiomers colored according to Figure 3b as capped-stick models. One cage each is shown as space-fill model in element colors.

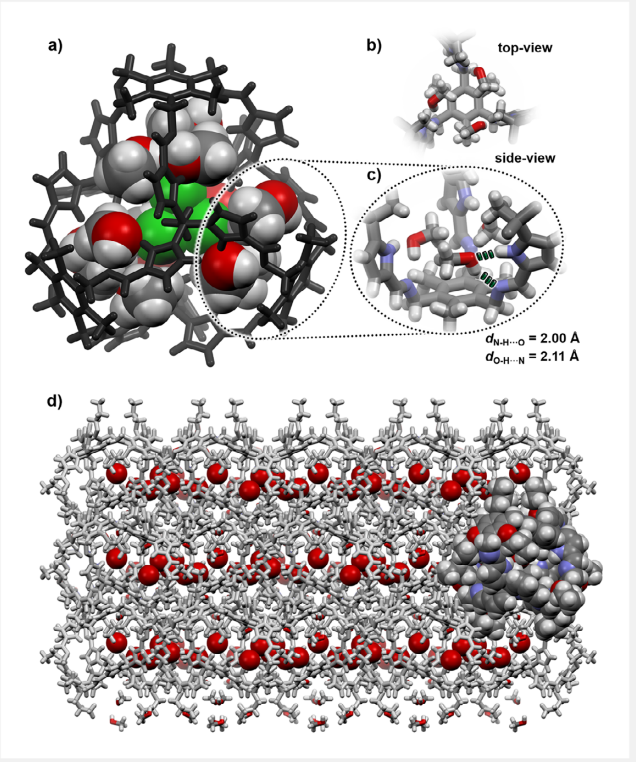

Figure 6 Residual solvent analysis of single-crystal X-ray structures of cages **3-Me** and **3-OPr**. a) Cage **3-Me** (shown in black as capped-stick model) with 12 molecules of methanol and one molecule of $CHCl_3$ (shown as space-fill models). b) Top-view and c) side-view of the hydrogen bonding pattern in detail. d) Crystal packing of cage **3-OPr** (shown as capped-stick models in white with one molecule shown as space-fill model in element colors) with ten methanol molecules (shown as capped-stick model in element colors) and ten water molecules (shown as a space-fill model in red without hydrogen atoms).

PPPP and *MMMM* cages in four cases and only cage **3-Et** can be found in the heteroenantiomeric *MMMP* and *PPPM* form in two solvates in the solid state. Furthermore, the nitrogen-rich interior of the cages is able to interact with polar molecules such as methanol or water and defined alignments like methanol shells or hydrogen-bonded chain-like structures were obtained. These findings can be beneficial for applications of the cages in the selective binding of polar guests or proton conductivity.[63–65] Furthermore, the nitrogen-rich cavity can be used as a cage ligand for transition metal ions or clusters.[66–69]

Funding Information

We thank the European Research Council (ERC) in the frame of the consolidator grant CaTs n DOCs (grant no. 725765) and Deutsche Forschungsgemeinschaft (DFG) under Germany's Excellence Strategy Cluster 3D Matter Made to Order (EXC-2082/1 – 390761711) for funding this project. The authors acknowledge support by the state of Baden-Württemberg through bwHPC and the German Research Foundation (DFG) through grant no. INST 40/575 – 1 FUGG (JUSTUS 2 cluster).

Acknowledgment

K.T. is grateful to the Chinese Scholarship Council for his PhD scholarship. M.P.S. is grateful to the Fond der Chemischen Industrie (FCI) for a Kekulé PhD scholarship. Tobias Kirschbaum is acknowledged for creating the models of the cages.

Supporting Information

Supporting Information for this article is available online at https://doi.org/10.1055/a-2041-5362.

Conflict of Interest

The authors declare no conflict of interest.

References

(1) Zhang, G.; Mastalerz, M. *Chem. Soc. Rev.* **2014**, *43*, 1934.
(2) Slater, A. G.; Cooper, A. I. *Science* **2015**, *348*, *6238*.
(3) Beuerle F.; Gole, B. *Angew. Chem. Int. Ed.* **2018**, *57*, 4850.
(4) Mastalerz, M. *Acc. Chem. Res.* **2018**, *51*, 2411.
(5) Little, M. A.; Cooper, A. I. *Adv. Funct. Mater.* **2020**, *30*, 1909842.
(6) Alexandre, P.-E.; Zhang, W.-S.; Rominger, F.; Elbert, S. M.; Schröder, R. R.; Mastalerz, M. *Angew. Chem. Int. Ed.* **2020**, *59*, 19675.
(7) Brutschy, M.; Schneider, M. W.; Mastalerz, M.; Waldvogel, S. R. *Adv. Mater.* **2012**, *24*, 6049.
(8) Brutschy, M.; Schneider, M. W.; Mastalerz, M.; Waldvogel, S. R. *Chem. Commun.* **2013**, *49*, 8398.
(9) Lauer, J.; Bhat, A.; Barwig, C.; Fritz, N.; Kirschbaum, T.; Rominger, F.; Mastalerz, M. *Chem. Eur. J.* **2022**, *28*, e202201527.
(10) Bushell, A. F.; Budd, P. M.; Attfield, M. P.; Jones, J. T. A.; Hasell, T.; Cooper, A. I.; Bernardo, P.; Bazzarelli, F.; Clarizia, G.; Jansen, J. C. *Angew. Chem. Int. Ed.* **2013**, *52*, 1253.
(11) He, A.; Jiang, Z.; Wu, Y.; Hussain, H.; Rawle, J.; Briggs, M. E.; Little, M. A.; Livingston, A. G.; Cooper, A. I. *Nat. Mater.* **2022**, *21*, 463.
(12) Zhang, G.; Presly, O.; White, F.; Oppel, I. M.; Mastalerz, M. *Angew. Chem. Int. Ed.* **2014**, *53*, 1516.
(13) Su, K.; Wang, W.; Du, S.; Ji, C.; Zhou, M.; Yuan, D. *J. Am. Chem. Soc.* **2020**, *142*, 18060.
(14) Martínez-Ahumada, E.; He, D.; Berryman, V.; López-Olvera, A.; Hernandez, M.; Jancik, V.; Martis, V.; Vera, M. A.; Lima, E.; Parker, D. J.; Cooper, A. I.; Ibarra, I. A.; Liu, M. *Angew. Chem. Int. Ed.* **2021**, *60*, 17556.
(15) Ivanova, S.; Köster, E.; Holstein, J. J.; Keller, N.; Clever, G. H.; Bein T.; Beuerle, F. *Angew. Chem. Int. Ed.* **2021**, *60*, 17455.
(16) Elbert, S. M.; Rominger F.; Mastalerz, M. *Chem. Eur. J.* **2014**, *20*, 16707.

(17) Hasell, T.; Miklitz, M.; Stephenson, A.; Little, M. A.; Chong, S. Y.; Clowes, R.; Chen, L.; Holden, D.; Tribello, G. A.; Jelfs, K. E.; Cooper, A. I. *J. Am. Chem. Soc.* **2016**, *138*, 1653.
(18) Elbert, S. M.; Regenauer, N. I.; Schindler, D.; Zhang, W.-S.; Rominger, F.; Schröder, R. R.; Mastalerz, M. *Chem. Eur. J.* **2018**, *24*, 11438.
(19) Liu, M.; Zhang, L.; Little, M. A.; Kapil, V.; Ceriotti, M.; Yang, S.; Ding, L.; Holden, D. L.; Balderas-Xicohténcatl, R.; He, D.; Clowes, R.; Chong, S. Y.; Schütz, G.; Chen, L.; Hirscher, M.; Cooper, A. I. *Science* **2019**, *366*, 613.
(20) Tian, K.; Elbert, S. M.; Hu, X.-Y.; Kirschbaum, T.; Zhang, W.-S.; Rominger, F.; Schröder, R. R.; Mastalerz, M. *Adv. Mater.* **2022**, *34*, 2202290.
(21) Liu, C.; Liu, K.; Wang, C.; Liu, H.; Wang, H.; Su, H.; Li, X.; Chen, B.; Jiang, J. *Nat. Commun.* **2020**, *11*, 1047.
(22) Kewley, A.; Stephenson, A.; Chen, L.; Briggs, M. E.; Hasell T.; Cooper, A. I. *Chem. Mater.* **2015**, *27*, 3207.
(23) Zhang, J.-H.; Xie, S.-M.; Chen, L.; Wang, B.-J.; He, P.-G.; Yuan, L.-M. *Anal. Chem.* **2015**, *87*, 7817.
(24) Koo, J.; Kim, I.; Kim, Y.; Cho, D.; Hwang, I.-C.; Mukhopadhyay, R. D.; Song, H.; Ko, Y. H.; Dhamija, A.; Lee, H.; Hwang, W.; Kim, S.; Baik, M.-H.; Kim, K. *Chem*, **2020**, *6*, 3374.
(25) Santolini, V.; Miklitz, M.; Berardo, E.; Jelfs, K. E. *Nanoscale* **2017**, *9*, 5280.
(26) Schneider, M. W.; Oppel, I. M.; Griffin, A.; Mastalerz, M. *Angew. Chem. Int. Ed.* **2013**, *52*, 3611.
(27) Mastalerz, M. *Angew. Chem. Int. Ed.* **2010**, *49*, 5042.
(28) Lauer, J. C.; Zhang, W. S.; Rominger, F.; Schröder, R. R.; Mastalerz, M. *Chem. Eur. J.* **2018**, *24*, 1816.
(29) Kunde, T.; Nieland, E.; Schröder, H. V.; Schalley, C. A.; Schmidt, B. M. *Chem. Commun.* **2020**, *56*, 4761.
(30) Skowronek, P.; Gawronski, J. *Org. Lett.* **2008**, *10*, 4755.
(31) Tozawa, T.; Jones, J. T. A.; Swamy, S. I.; Jiang, S.; Adams, D. J.; Shakespeare, S.; Clowes, R.; Bradshaw, D.; Hasell, T.; Chong, S. Y.; Tang, C.; Thompson, S.; Parker, J.; Trewin, A.; Bacsa, J.; Slawin, A. M. Z.; Steiner, A.; Cooper, A. I. *Nat. Mater.* **2009**, *8*, 973.
(32) Jiao, T.; Chen, L.; Yang, D.; Li, X.; Wu, G.; Zeng, P.; Zhou, A.; Yin, Q.; Pan, Y.; Wu, B.; Hong, X.; Kong, X.; Lynch, V. M.; Sessler, J. L.; Li, H. *Angew. Chem. Int. Ed.* **2017**, *56*, 14545.
(33) Cao, N.; Wang, Y.; Zheng, X.; Jiao, T.; Li, H. *Org. Lett.* **2018**, *20*, 7447.
(34) Jiang, S.; Bacsa, J.; Wu, X.; Jones, J. T. A.; Dawson, R.; Trewin, A.; Adams, D. J.; Cooper, A. I. *Chem. Commun.* **2011**, *47*, 8919.
(35) Schneider, M. W.; Oppel, I. M.; Mastalerz, M. *Chem. Eur. J.* **2012**, *18*, 4156.
(36) Acharyya, K.; Mukherjee, P. S. *Chem. Eur. J.* **2014**, *20*, 1646.
(37) Xu, D.; Warmuth, R. *J. Am. Chem. Soc.* **2008**, *130*, 7520.
(38) Wagner, P.; Rominger, F.; Zhang, W.-S.; Gross, J. H.; Elbert, S. M.; Schröder, R. R.; Mastalerz, M. *Angew. Chem. Int. Ed.* **2021**, *60*, 8896.
(39) Mukhopadhyay, R. D.; Kim, Y.; Koo, J.; Kim, K. *Acc. Chem. Res.* **2018**, *51*, 2730.
(40) Hong, S.; Rohman, M. R.; Jia, J.; Kim, Y.; Moon, D.; Kim, Y.; Ko, Y. H.; Lee, E.; Kim, K. *Angew. Chem. Int. Ed.* **2015**, *54*, 13241.
(41) Qu, H.; Wang, Y.; Li, Z.; Wang, X.; Fang, H.; Tian, Z.; Cao, X. *J. Am. Chem. Soc.* **2017**, *139*, 18142.
(42) Mastalerz, M. *Chem. Commun.* **2008**, 4756.
(43) Schneider, M. W.; Oppel, I. M.; Ott, H. L.; Lechner, G.; Hauswald, H.-J. S.; Stoll, R.; Mastalerz, M. *Chem. Eur. J.* **2012**, *18*, 836.
(44) Briggs, M. E.; Jelfs, K. E.; Chong, S. Y.; Lester, C.; Schmidtmann, M.; Adams, D. J.; Cooper, A. I. *Cryst. Growth Des.* **2013**, *13*, 4993.
(45) Bourguignon, C.; Schindler, D.; Zhou, G.; Rominger, F.; Mastalerz, M. *Org. Chem. Front.* **2021**, *8*, 3668.
(46) Hasell, T.; Wu, X.; Jones, J. T. A.; Bacsa, J.; Steiner, A.; Mitra, T.; Trewin, A.; Adams, D. J.; Cooper, A. I. *Nat. Chem.* **2010**, *2*, 750.
(47) Benke, B. P.; Kirschbaum, T.; Graf, J.; Gross, J. H.; Mastalerz, M. *Nat. Chem.* **2023**, *15*, 413.
(48) Hu, X.-Y.; Zhang, W.-S.; Rominger, F.; Wacker, I.; Schroder, R. R.; Mastalerz, M. *Chem. Commun.* **2017**, *53*, 8616.
(49) Bhat, A. S.; Elbert, S. M.; Zhang, W.-S.; Rominger, F.; Dieckmann, M.; Schröder, R. R.; Mastalerz, M. *Angew. Chem. Int. Ed.* **2019**, *58*, 8819.
(50) Wang, H.; Jin, Y.; Sun, N.; Zhang, W.; Jiang, J. *Chem. Soc. Rev.* **2021**, *50*, 8874.
(51) Wang, F.; Sikma, E.; Duan, Z.; Sarma, T.; Lei, C.; Zhang, Z.; Humphrey, S. M.; Sessler, J. L. *Chem. Commun.* **2019**, *55*, 6185.
(52) Oh, J. H.; Kim, J. H.; Kim, D. S.; Han, H. J.; Lynch, V. M.; Sessler, J. L.; Kim, S. K. *Org. Lett.* **2019**, *21*, 4336.
(53) Pilgrim, B. S.; Champness, N. R. *ChemPlusChem* **2020**, *85*, 1842.
(54) Zhang, D.; Ronson, T. K.; Nitschke, J. R. *Acc. Chem. Res.* **2018**, *51*, 2423.
(55) Beer, P. D.; Cheetham, A. G.; Drew, M. G. B.; Fox, O. D.; Hayes, E. J.; Rolls, T. D. *Dalton Trans.* **2003**, 603.
(56) Fox, O. D.; Rolls, T. D.; Drew, M. G. B.; Beer, P. D. *Chem. Commun.* **2001**, 1632.
(57) Wang, X.; Wang, Y.; Yang, H.; Fang, H.; Chen, R.; Sun, Y.; Zheng, N.; Tan, K.; Lu, X.; Tian, Z.; Cao, X. *Nat. Commun.* **2016**, *7*, 12469.
(58) Qu, H.; Huang, Z.; Dong, X.; Wang, X.; Tang, X.; Li, Z.; Gao, W.; Liu, H.; Huang, R.; Zhao, Z.; Zhang, H.; Yang, L.; Tian, Z.; Cao, X. *J. Am. Chem. Soc.* **2020**, *142*, 16223.
(59) Ubasart, E.; Borodin, O.; Fuertes-Espinosa, C.; Xu, Y.; García-Simón, C.; Gómez, L.; Juanhuix, J.; Gándara, F.; Imaz, I.; Maspoch, D.; von Delius, M.; Ribas, X. *Nat. Chem.* **2021**, *13*, 420.
(60) Zhang, D.; Ronson, T. K.; Greenfield, J. L.; Brotin, T.; Berthault, P.; Léonce, E.; Zhu, J.-L.; Xu, L.; Nitschke, J. R. *J. Am. Soc. Chem.* **2019**, *141*, 8339.
(61) Rousseaux, S. A. L.; Gong, J. Q.; Haver, R.; Odell, B.; Claridge, T. D. W.; Herz, L. M.; Anderson, H. L. *J. Am. Soc. Chem.* **2015**, *137*, 12713.
(62) Cai, K.; Lipke, M. C.; Liu, Z.; Nelson, J.; Cheng, T.; Shi, Y.; Cheng, C.; Shen, D.; Han, J.-M.; Vemuri, S.; Feng, Y.; Stern, C. L.; Goddard, W. A.; Wasielewski, M. R.; Stoddart, J. F. *Nat. Commun.* **2018**, *9*, 5275.
(63) Liu, M.; Chen, L.; Lewis, S.; Chong, S. Y.; Little, M. A.; Hasell, T.; Aldous, I. M.; Brown, C. M.; Smith, M. W.; Morrison, C. A.; Hardwick, L. J.; Cooper, A. I. *Nat. Commun.* **2016**, *7*, 12750.
(64) Hu, D.; Zhang, J.; Liu, M. *Chem. Commun.* **2022**, *58*, 11333.
(65) Montà-González, G.; Sancenón, F.; Martínez-Máñez, R.; Martí-Centelles, V. *Chem. Rev.* **2022**, *122*, 13636.
(66) Chakraborty, D.; Mukherjee, P.S. *Chem. Commun.* **2022**, *58*, 5558.
(67) McCaffrey, R.; Long, H.; Jin, Y.; Sanders, A.; Park, W.; Zhang, W. *J. Am. Soc. Chem*, **2014**, *136*, 1782.
(68) Song, Q.; Wang, W. D.; Hu, X.; Dong, Z. *Nanoscale*, **2019**, *11*, 21513.
(69) Du, Y.-J.; Zhou, J.-H.; Tan, L.-X.; Liu, S.-H.; Zhao, K.; Gao, Z.-M.; Sun, J.-K. *ACS Appl. Nano Mater.* **2022**, *5*, 7974.